How few cancer cells can be detected by positron emission tomography? A frequent question addressed by an in vitro study

Barbara M. Fischer[1], Minna W. B. Olsen[2], Carsten D. Ley[2], Thomas L. Klausen[3], Jann Mortensen[1], Liselotte Højgaard[1], Paul E. G. Kristjansen[2]

[1] Department of Clinical Physiology, Nuclear Medicine and PET, Copenhagen University Hospital, Copenhagen, Denmark
[2] Laboratory of Experimental Oncology, Molecular Pathology, University of Copenhagen, Copenhagen, Denmark
[3] Department of Clinical Physiology, Herlev University Hospital, DK-2730 Herlev, Denmark

Received: 29 June 2005 / Accepted: 8 November 2005 / Published online: 13 April 2006

Abstract. *Purpose:* Positron emission tomography (PET) has gained widespread use in cancer diagnosis and treatment, but how many malignant cells are required for a tumour to be detected by PET?
Methods: Three human cancer cell lines [glioblastoma and two subtypes of small cell lung cancer (SCLC)] in concentrations from 10^4 to 10^7 were seeded on six-well plates or plastic tubes and treated with [^{18}F]fluorodeoxyglucose (FDG) in vitro. FDG retention was measured in a PET/CT scanner and in a calibrated well counter. The clinical situation was simulated using a cylinder phantom with a background concentration of FDG.
Results: The theoretical detection limit was found to be around 10^5 malignant cells. In a cylinder phantom the detection limit was increased by a factor of 10. The FDG retention by the glioblastoma cell line was significantly higher than the activity of the SCLC cell line. FDG retention measured by PET and a gamma counter was closely correlated to the number of cells and a linear relationship was found.
Discussion: The detection limit of PET is in the magnitude of 10^5 to 10^6 malignant cells. The experimental set-up was robust and well suited as a platform for further investigations of factors influencing the detection limit of PET.

Keywords: Positron emission tomography – Detection limit – Cancer – Malignant cells – Number

Eur J Nucl Med Mol Imaging (2006) 33:697–702
DOI 10.1007/s00259-005-0038-6

The first two named authors contributed equally to this paper.

Barbara M. Fischer (✉)
Department of Clinical Physiology, Nuclear Medicine and PET,
Copenhagen University Hospital,
Copenhagen, Denmark
e-mail: malene.fischer@rh.dk
Tel.: +45-35454011, Fax: +45-35453898

Introduction

Positron emission tomography (PET) has gained widespread use in the diagnosis and staging of cancer, as well as in treatment planning and evaluation. In this respect, [^{18}F]fluorodeoxyglucose (FDG) is by far the most commonly used PET tracer, exploiting the increased glucose uptake and metabolism in malignant cells [1]. ^{18}F decays by positron emission followed by annihilation under emission of two 511-keV photons. Movement of the positron before annihilation and slight variations in the angle between the two photons limit the spatial resolution of clinical PET [2]. Current clinical systems are capable of 4–5 mm spatial resolution, and evidence for the sensitivity of PET in detecting tumours smaller than 10 mm is now emerging [3, 4].

Accurate diagnosis of a tumour by PET is not only dependent on the anatomical size: the metabolism of the specific cancer cells, the localisation of the tumour, the uptake of FDG in the surrounding tissue and the number of viable malignant cells in the tumour are all decisive. Most of these factors are well described, but in this study we set out to answer the apparently simple question: How many malignant cells are required for a tumour to be detected by FDG-PET?

Materials and methods

Cell lines

Three human cancer cell lines were used in the study: two subtypes of small cell lung cancer (SCLC) cell lines, CPH54A and CPH54B [5] and one glioblastoma cell line, U373. Cells were grown in monolayer and maintained in modified Eagle's medium (Gibco BRL) without antibiotics under standard cell culture conditions.

Detection limit experiment

Twenty-four hours prior to the experiments, duplicate wells containing 10^4, 10^5 and 10^6 cells of the cell lines CPH54B and

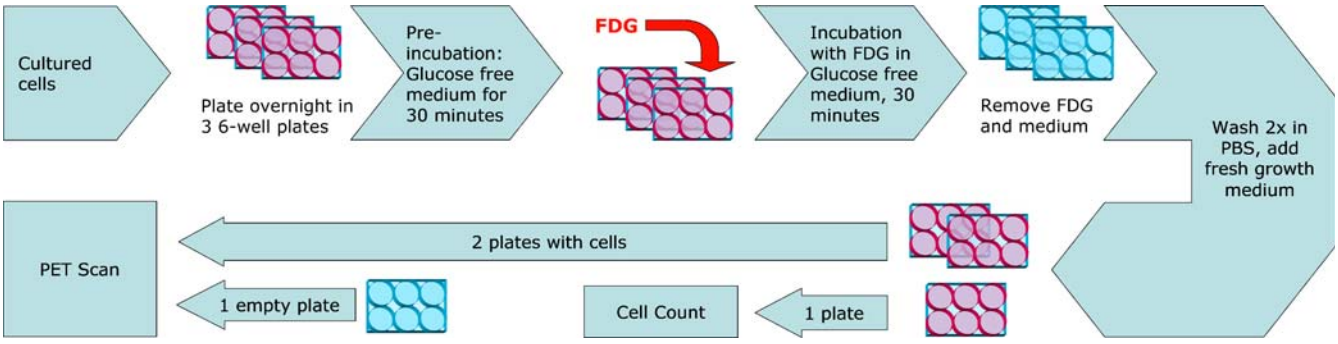

Fig. 1. Preparation of six-well plates for the detection limit experiment

U373 were seeded on three six-well plates each and allowed to attach (Fig. 1). Prior to treatment with FDG the cells were incubated with glucose-free medium for 30 min. FDG corresponding to an activity of 0.1 MBq/ml at scan time was added to each well. After incubation with FDG for 30 min, the cells were washed twice with phosphate-buffered saline and 3 ml of fresh growth medium was added to each well [6]. Two six-well plates with each cell line were scanned, together with an empty control plate not treated with FDG. Cells from the third six-well plate were harvested and counted in a haemocytometer.

Cell quantification experiment

In order to explore the possibility of quantification by FDG-PET, cells were seeded in cell culture flasks (Fig. 2). Growth medium was removed and 25 ml of glucose-free medium was added. Cells were pre-incubated for 30 min, before an FDG dose corresponding to 0.1 MBq/ml at scan time was added to the glucose-free medium. FDG and medium were removed after 30 min; cells were washed in PBS, harvested and counted. Appropriate cell numbers were transferred to test tubes, and growth medium was topped up to a total volume of 3 ml in each tube. CPH54A cells (0, 10^4, 5×10^4, 10^5, 5×10^5, 10^6, 2×10^6, 5×10^6, and 10^7 cells per tube) were evaluated in a well counter and then PET scanned. This experiment was repeated four times to assure reproducibility. U373 cell (10^4, 10^5 and 10^6 cells per tube) were placed in the cylinder phantom and PET scanned to simulate a clinical setting with background radiation (4.1 MBq/l at scan time).

Quantification of FDG retention

FDG retention was measured in a PET/CT scanner (GE Discovery, General Electric Medical Systems, Milwaukee, WI, USA), with a maximal spatial resolution of 4 mm, an image matrix of 256×256 and a pixel size in reconstructed images of 1×1 mm^2. Using a static PET scan, each six-well plate was measured for 5 min. CT scan (140 kV and 10 mA) was used for attenuation correction. PET raw data were reconstructed using ordered subset expectation maximisation (OSEM, 2 iterations, 28 subsets, port filter 6 mm).

A separate experiment was performed in order to test the sensitivity of the equipment. Activity could be visualised (5-min frame) by the PET/CT scanner when the concentration in one well was as low as 50 Bq/ml; the very smallest amount of activity detectable by the PET/CT scan is even lower (<10 Bq). Similarly, in the well counter the background radiation was below 20 cpm, and we therefore had sensitivity down to 1 Bq.

It was verified that a surplus of FDG was offered to the cells by a 12-h emission scan; thus the offered amount of FDG was not a limiting factor for the FDG uptake.

A region of interest (ROI) was defined over each well (ROI size of 10 cm^2, Fig. 3) or tube (ROI size of 3 cm^2, Fig. 5) and the FDG retention as average Bq/cc (becquerels per cubic centimetre) was determined. The average retention of FDG by a single cell was estimated by dividing the decay-corrected uptake (Bq/cc) with the actual number of cells counted in a haemocytometer (cells/cc). The tubes containing CPH54A cells for the quantification study were also evaluated for 1 min in a calibrated well counter (Cobra II gamma counting system, model 5003; Packard, Meriden, CT, USA). Results are

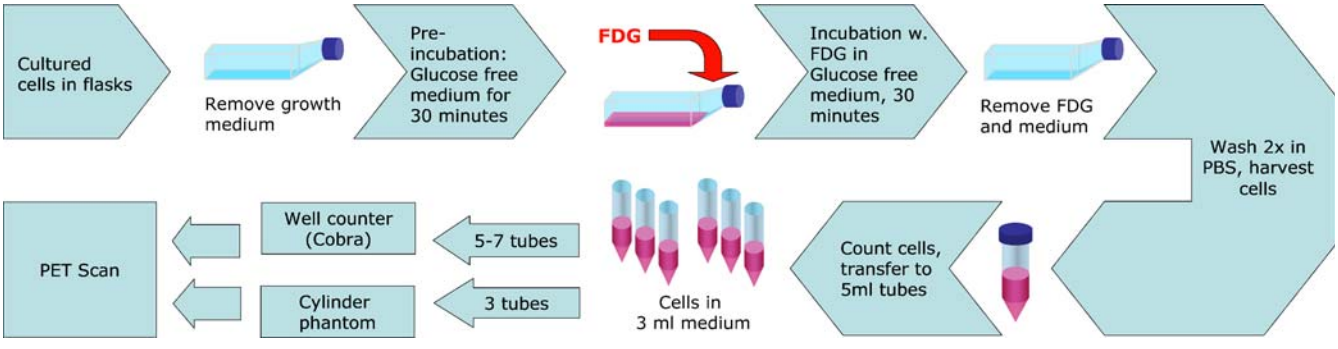

Fig. 2. Experimental set-up for cell quantification and scanning in cylinder phantom

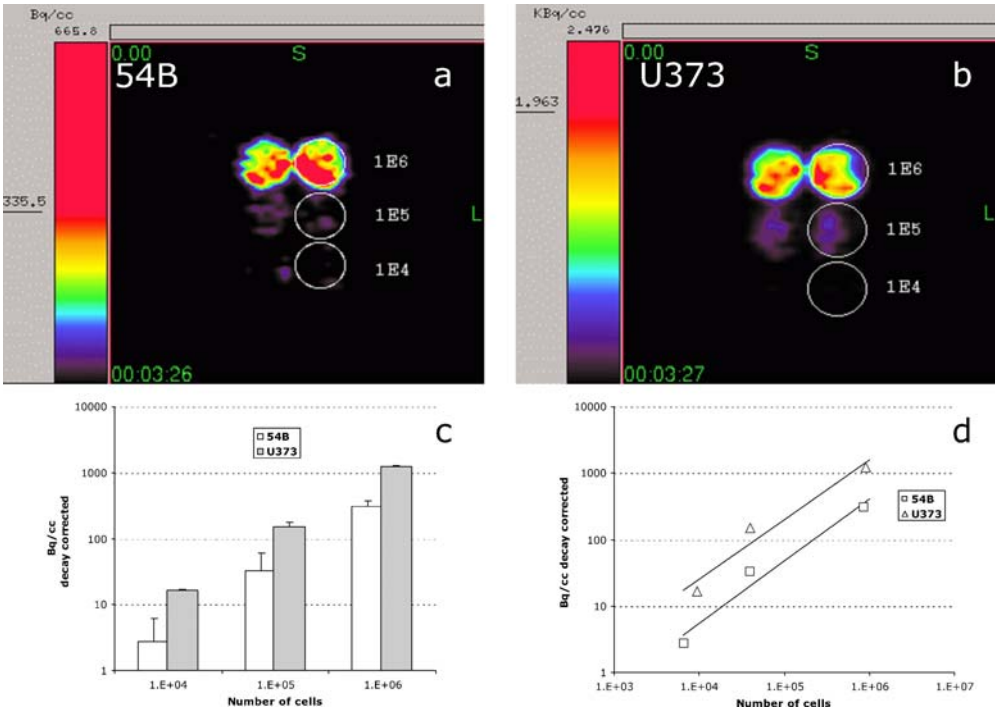

Fig. 3. a,b Coronal PET images of six-well trays with CPH54B and U373 cells in three different concentrations. ROI shown over the right row of wells. **c** Average retention of FDG per volume by CPH54B and U373. FDG retention reported as Bq/cc from coronal PET images. Results are decay corrected and shown on a log scale. *Error bars* represent one standard deviation. **d** Average retention of FDG by CPH54B and U373 correlated significantly with the actual number of cells in each well (shown on double log-scale; r_s=1.00, p<0.01 for both cell lines). For a more similar weighting of all observations, coordinates were log-transformed before linear regression analysis. Good linearity was found: r^2 equals 0.97 for CPH54B and 0.95 for U373

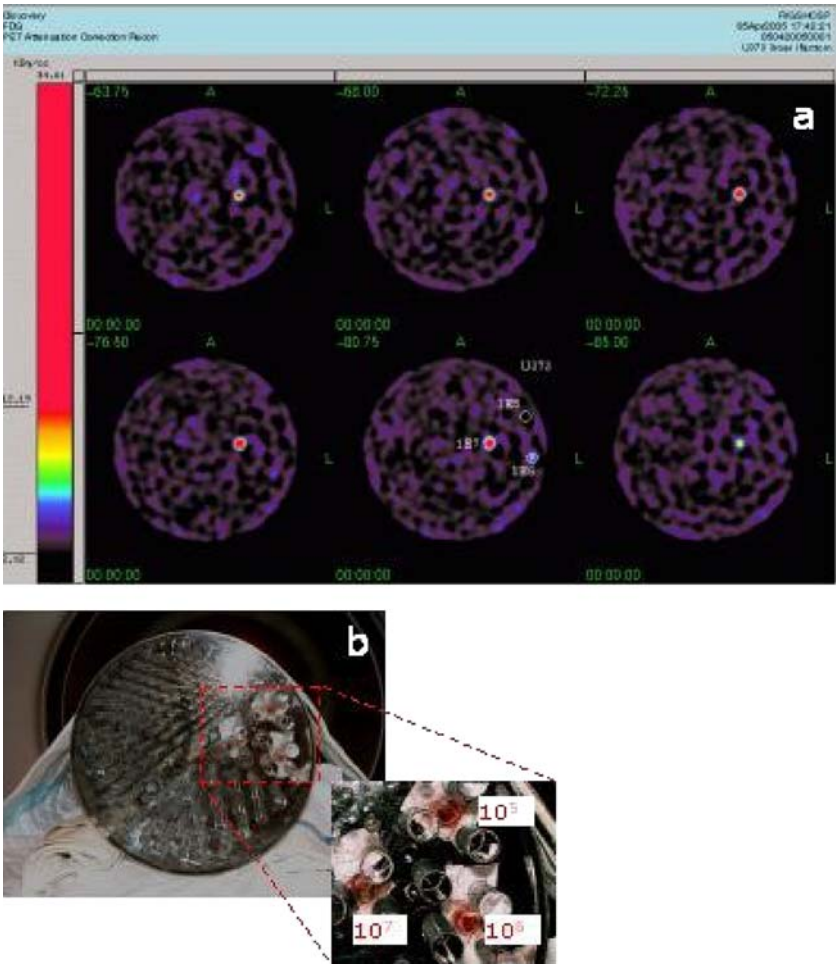

Fig. 4. a Transaxial PET images of cylinder phantom with tubes containing 10^5, 10^6 and 10^7 cells (U373). The tube with 10^7 cells is visible on all shown slices; 10^5 cells is not visible in this set-up. **b** Photo of cylinder phantom, placed in PET/CT scanner, with tubes containing 10^5, 10^6 and 10^7 cells

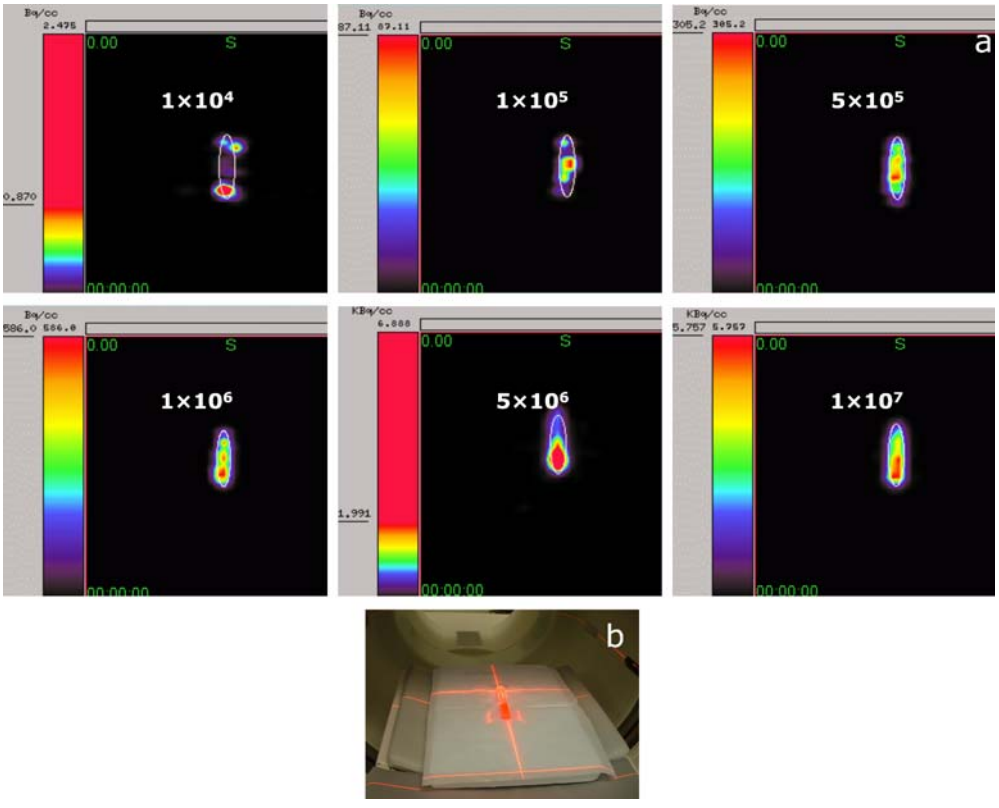

Fig. 5. a Coronal PET images of FDG uptake by 10^4–10^7 CPH54A cells. ROI corresponding to each tube is shown. **b** Photo of a tube placed in the PET/CT scanner

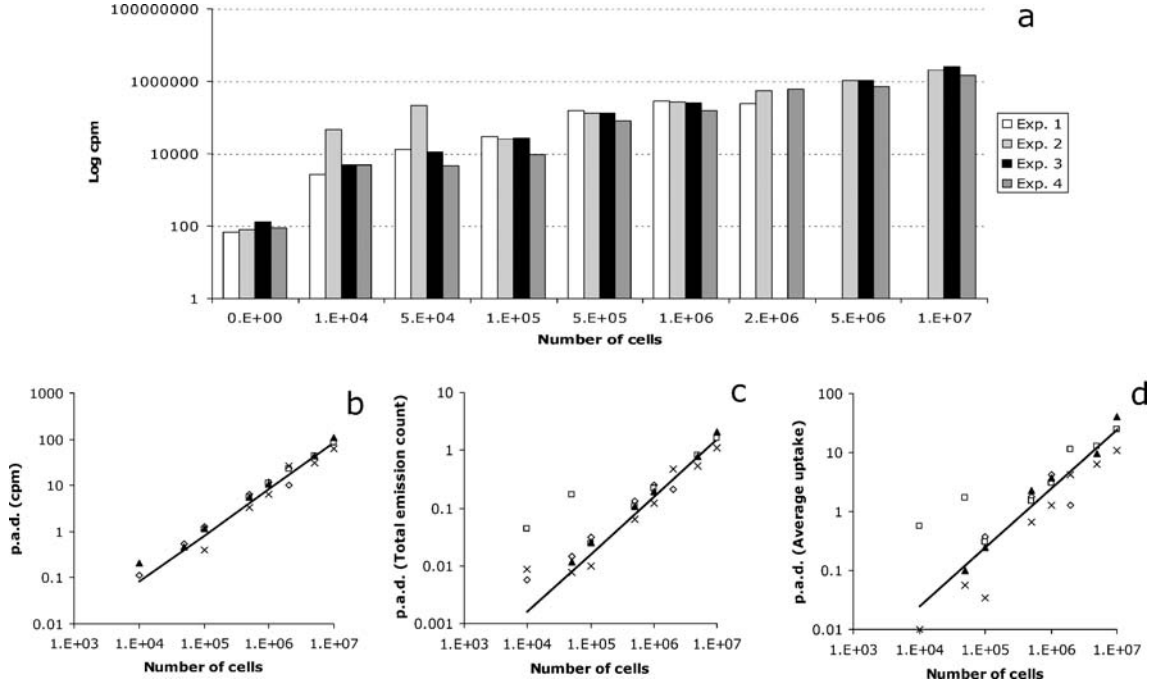

Fig. 6. a Results from each experiment (tubes with CPH54A) shown as cpm on log scale. **b** Significant correlation (r_s=0.95, p<0.001) and linearity (r^2=0.93) between number of cells and cpm from gamma counter (normalised as percent of added dose per volume (p.a.d.) on log scale). *c* Significant correlation (r_s=0.83, p<0.001) and linearity (r^2=0.92) between number of cells and total emission counts from PET/CT (normalized as p.a.d.) on log scale. **d** Significant correlation (r_s=0.83, p<0.001) between number of cells and average uptake per volume estimated from PET images (normalized as p.a.d.), shown on log scale. Linearity was less convincing: r^2=0.74

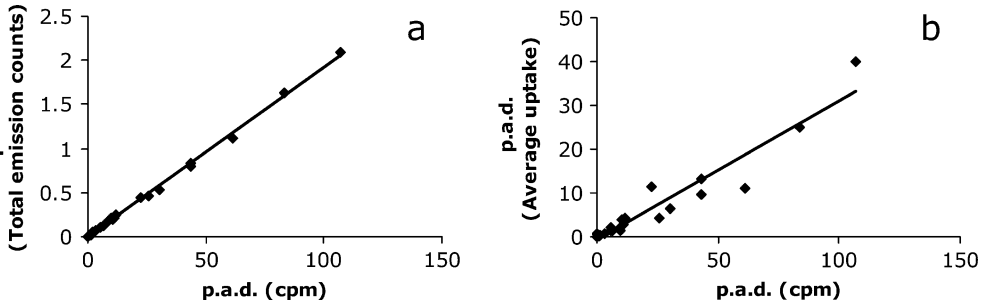

Fig. 7. a Linear correlation (r^2=0.99) between results obtained in a gamma counter and total emission counts from PET. **b** Linear correlation (r^2=0.92) between results obtained in a gamma counter and average retention from PET images

reported as counts per minute (cpm). Signals detected by PET imaging and gamma counting were decay corrected and normalised to the amount of FDG initially added per volume. Therefore, the FDG retention can be compared between experiments and cell lines; these results are presented as p.a.d. (percent of added dose per volume).

Finally, tubes with U373 in numbers of 10^5, 10^6 and 10^7 were scanned in a cylinder (diameter 216 mm) phantom (Hot Spot, Data Spectrum, Hillsborough, NC, USA). After insertion of the tubes the phantom was filled with distilled water (6.1 l) and 25 MBq of FDG was added immediately prior to the PET scan. This background concentration of 4.1 MBq/l imitates the background in a 70-kg patient treated with 400 MBq 1 h prior to PET scanning (assuming that the decay-corrected activity is equally distributed in the patient) [7].

Statistical analysis was performed using non-parametric statistics (Mann Whitney, two-tailed analysis). Significance of correlation was tested by Spearman's ρ (r_s) and linearity was estimated from the correlation coefficient determined by linear regression (r^2).

Results

Detection limit

In this experiment, the number of cells corresponding to the detection limit of the PET scanner was investigated, and the results are presented in Fig. 3. Coronal images and quantification of six-well plates with the cell lines CPH54B and U373 are shown in Fig. 3a and b. The retention of FDG by the two cell lines is visibly different. The wells with a monolayer of 10^5 cells are visually different from the background, although this is more obvious for U373 than for CPH54B. Fig. 3c presents the average decay-corrected retention of FDG for the cell lines. The average activity in the wells containing 10^5 cells is significantly higher than the background in both cell lines (p<0.05). In the wells with 10^4 cells, we did not detect activity significantly above background levels. The activity of U373 cells was significantly higher (p<0.03) than that of CPH54B cells. In Fig. 3d, the FDG retention by U373 and CPH54B is related to the actual number of cells counted in each well on the third plate (not scanned). The average retention by a single U373 cell was 0.015 Bq, whereas it was 0.003 for a CPH54B cell. We found FDG retention and the number of cells to be correlated (r_s=1.00, p<0.01) for both cell lines. Correlation coefficients r^2=0.97 (CPH54B) and r^2=0.95 (U373) indicated a linear relationship, from which the theoretical detection limit can be estimated.

Figure 4 shows transaxial PET images of tubes with U373 cells, placed in a cylinder phantom simulating typical background radiation from a human body. In this situation, only the tubes with 10^6 and 10^7 cells are visible, indicating a clinical detection limit of around 10^6 cells.

Cell quantification

The aim of this experiment was to demonstrate a linear relationship between the number of tumour cells and FDG retention, as well as the agreement between different evaluation methods. Figure 5 presents PET images of different numbers of CPH54A cells in tubes containing growth medium; 10^5 was the smallest number of cells that could readily be imaged.

This experiment was repeated on four different occasions, and as demonstrated in Fig. 6a, the results were robust from experiment to experiment. A significant correlation between cell number and FDG retention was found regardless of the detection method, as shown in Fig. 6b–d (p<0.001). Cell numbers and FDG retention evaluated by a gamma counter showed a good linear correlation (r^2=0.93). Cell numbers and FDG retention evaluated by total emission counts in the PET scanner also correlated in a linear fashion (r^2=0.92). However, the linearity between cell numbers and the signal detected on PET images was less convincing (r^2=0.74). As the latter method only includes counts from the manually drawn ROI, complete correlation cannot be expected. Similarly, we observed good linearity between measurements of FDG retention by gamma counter and by total emission counts in the PET scanner (Fig. 7a), whereas the correlation between results from the gamma counter and signal detected on PET images was less robust (Fig. 7b).

Discussion

In this study, the detection limit of FDG-PET was examined by scanning cancer cells treated with FDG in vitro. Our findings indicate that the theoretical detection limit of the present FDG-PET technology is in the magnitude of 10^5 tumour cells, depending on the glucose turnover of the specific cancer. Differences in glucose metabolism between the SCLC and glioblastoma cell lines

were apparent. We estimate that such differences may influence the detection limit by a factor of 5–10.

We also presented a method for quantification of cell numbers by FDG-PET: The number of cancer cells correlated with the FDG retention, regardless of whether it was determined by gamma counter, total emission counts in the scanner or average retention on PET images. This, and the reproducibility of our observations, confirms that our experimental set-up is a reasonable model for estimation of number of cancer cells by FDG-PET.

These findings could be valuable when designing in vitro studies to evaluate the effect of new anti-cancer drugs on FDG retention by malignant cells. In principle, cell death (i.e. metabolic arrest) can be estimated from the results obtained by the gamma counter or PET. However, the relationship between the number of viable cells and FDG retention can vary substantially depending on the cancer cells, and especially in relation to differences in glucose metabolism. Our findings are in good agreement with results from a different set-up [8] describing the correlation between PET signal and cell number by a non-FDG strategy. The use of FDG, widely employed in different clinical settings, makes our study relevant to cancer diagnostics.

A clinical setting was simulated using a cylinder phantom with background radiation; this increased the detection limit by a factor of approximately 10. We expect similar results in patients, corresponding to a detection limit in the magnitude of 10^6 cells, depending on the specific cancer studied. Findings in a casuistic report are in agreement with this [9]. An approach to the differences in detection limit due to the specific uptake of FDG by different cell lines could be to tailor the FDG dose, uptake and scan time according to the specific cell type in question. Whether this would be relevant and feasible could be a subject for future studies. The diameter of a tumour of 10^6 cells is approximately 1 mm [10], just detectable by CT but below the spatial resolution of present PET technology. However, as indicated by our results, such a small tumour could still be detectable by PET. This strengthens the theoretical relevance of PET, e.g. for screening purposes. Furthermore, it indicates that the detection limit of a PET/CT scanner is in the range of another emerging FDG technology—intraoperative positron probe (sensitivity 2.6 cps/kBq, ability to distinguish FDG-avid areas <5 mm) [11, 12].

Conclusion

The detection limit of PET is in the magnitude of 10^5 to 10^6 malignant cells, provided that the minimum uptake of FDG corresponds to an activity of approximately 50 Bq/ml. In a clinical setting, the detection limit is estimated to be 10 times larger, but still below the spatial resolution of PET. The detection limit varies by a factor of 5–10 according to the glucose metabolism of the specific cell type in question. The experimental set-up described in this study is well suited as a platform for further investigations of factors influencing the detection limit of PET, e.g. respiratory movement, density, size and therapy.

Acknowledgement. The authors wish to thank technologist Susanne Svalling for her invaluable and competent assistance during this project.

References

1. Pauwels EKJ, Sturm EJC, Bombardieri E, Cleton FJ, Stokkel MPM. Positron-emission tomography with [^{18}F]fluorodeoxyglucose. Part I. Biochemical uptake mechanism and its implication for clinical studies. J Cancer Res Clin Oncol 2000;126:549–559
2. Cherry SR, Phelps ME. Positron emission tomography: methods and instrumentation. In: Sandler MP, et al, editors. Diagnostic nuclear medicine, volume 1. Baltimore: Williams and Wilkins; 1995; p. 139–159
3. Vansteenkiste JF, Stroobants SG. The role of positron emission tomography with ^{18}F-fluoro-2-deoxy-D-glucose in respiratory oncology. Eur Respir J 2001;17:802–820
4. Ho Shon I, O'Doherty MJ, Maisey MN. Positron emission tomography in lung cancer. Semin Nucl Med 2002;32(4):240–270
5. Pedersen MWB, Holm S, Lund EL, Højgaard L, Kristjansen PEG. Coregulation of glucose uptake and vascular endothelial growth factor (VEGF) in two small-cell lung cancer (SCLC) sublines in vivo and in vitro. Neoplasia 2001;3(1):80–87
6. Haberkorn U, Morr I, Oberdorfer F, Bellemann ME, Blatter J, Altmann A, et al. Fluorodeoxyglucose uptake in vitro: aspects of method and effects of treatment with gemcitabine. J Nucl Med 1994;35(11):1842–1850
7. Raylman RR, Wahl RL. Evaluation of ion-implanted-silicon detectors for use in intraoperative positron-sensitive probes. Med Phys 1996;23(11):1889–1895
8. Su H, Forbes A, Gambhir SS, Braun J. Quantitation of cell number by a positron emission tomography reporter gene strategy. Mol Imaging Biol 2004;6(3):139–148
9. Ruf J, Amthauer H, Oettle H, Steinmüler T, Plotkin M, Pelzer U, et al. Role of F18-FDG PET for monitoring of radiochemotherapy—estimation of detectable number of tumour cells. Onkologie 2004;27:287–290
10. Geddes DM. The natural history of lung cancer: a review based on rates of tumour growth. Br J Dis Chest 1979;73(1):1–17
11. Raylman RR, Srinivasan A. Endoprobe: a system for radionuclide-guided endoscopy. Med Phys 2004;31(12):3306–3313
12. Yamamoto S, Matsumoto K, Sakamoto S, Tarutani K, Minato K, Senda M. An intra-operative positron probe with background rejection capability for FDG guided surgery. Ann Nucl Med 2005;19(1):23–28